While human patients and healthy subjects are being imaged at 3T, 7T, and soon, 10.5T, more data and understanding of RF safety at these ultra-high field strengths are needed. The overall objective of this renewal proposal therefore is to extend the RF heating studies in the human head of our previous grant to the investigation of RF heating in the human body for ultra-high field MRI applications. Safety will be better assured and imaging performance improved by developing the means to accurately predict and measure RF temperature contours in human anatomy. Through development of new theory, technology, methodology, and experimental approach, these means will be achieved by accomplishing the following aims. First, a more fundamental understanding of the electrodynamics and thermodynamic nature of RF induced heating and heat transfer in anatomy will be furthered through mechanistic improvement of the empirical Pennes Bioheat Equation. Second, this new theoretical model will be validated at high field Larmor frequencies by invasive, direct measurement of RF heating in anesthetized porcine models, by fluoroptic thermometry. The porcine model is required as an intermediate step toward understanding and measuring RF heating in humans. Toward this end, the third aim is to develop a noninvasive NMR thermometer that is accurately and precisely calibrated by the invasive fluoroptic measurement. Once confidence is gained in predicting and noninvasively measuring temperatures in pigs, these methods will be applied or correlated to monitoring RF heating in humans and so accomplishing the final aim of this study. With new understanding, data, and thermal measurement methods, high field human MRI will become safer.

While humans are being imaged at 3T, 7T, and soon, 10.5T, more data and understanding of RF safety at these ultra-high field strengths are needed. These RF safety issues were investigated for head imaging in the previous grant. The objective of this renewal proposal therefore is to continue the investigation of high frequency RF heating in the human body to improve RF safety and imaging performance for ultra-high field MRI. Safety will be better assured by developing means to accurately predict and image RF heating contours in human anatomy.

INTRODUCTION:

The investigators wish to thank the reviewers for their attention to the review of this proposal. The critiques received were individually considered and incorporated into a stronger revision. Accordingly much of the proposal was rewritten, obviating denotation of specific changes. While space here limits comprehensive response to the Summary Statement, concerns listed are addressed in the revised RESEARCH STRATEGY.

Receiving an enthusiastic review, the parent grant of this renewal was funded with a 1.9% score. The first try for this renewal proposal "was considered well organized and with complimentary aims and clear deliverables," for which "a successful outcome could significantly impact the ability to use high field MR." Also according to the Summary Statement, "The applicants were very productive in the prior funding period." The four reviewers gave averaged priority scores of 1.5, 1.5, and 1.0 respectively for "Significance," "Investigators" and "Environment." Because these were positive reviews, attention and page space will be devoted to the categories eliciting greater concern, namely "Approach" receiving an averaged score of 3.0 and "Innovation" with a score of 3.5.

Innovation: Critiques scored "Innovation" from 1.0 to 6.0. Reviewer 1 whose Innovation score = 6, questioned, "What's new?" The investigators' answer is manifold. 1.) Compared to the parent grant's focus solely on head imaging, this proposal extends to measure temperature over the whole body. 2.) This proposal improves on bioheat models and develops new temperature measurements to compensate for physiologic motion in the body. 3.) And it proposes new alternative thermal imaging methods with motion correction and TmDOTA reagent to correct for the originally proposed T1Rho methods that did not work for temperature measurements in the parent grant. 4.) Whole body imaging at 3T, 7T, and 10.5T, with single and dual tuned body coils is a highly innovative set of procedures and technology as well. Reviewers 2-4 noted additional innovations. Reviewer 2 (score =2) listed "new bioheat model" and "NMR thermometry improvements" as Innovation strengths and listed no weaknesses. Reviewer 3 (score = 1) agreed that "validation of theoretical bioheat transfer model with an MR thermometry method" and "new coil…at 10.5T" were notable Innovations, and listed no weaknesses in this category. Reviewer 4 (score=3) listed Innovative strengths as 1.) "strong in prior grant and still needed (in this grant)," 2.) "equations," and 3.) "MR-based porcine tissue model." The only weakness listed asked for more discussion on the bioheat equation which is included in this revision.

Approach: Critiques scored "Approach" from 2.0 to 5.0. Reviewer 1, with score = 5, agreed (strength) that "the move from modeling through validation in pigs through to humans again seems appropriate." This reviewer's weaknesses paraphrased were 1.) "Why no budget for 10.5T?" 2.) Why no experiments on 9.4T/65cm system?"and 3.) A backup plan should be included " if 10.5T system doesn't work out." The answers are respectively 1.) 10.5T imaging time was not included in the budget because it was not necessary or planned for imaging temperature generated by 450 MHz. The double tuned body coil was proposed for heating at 450 MHz with thermal imaging performed at 3T and/or 7T. In deference to the Reviewers' interest in a 10.5T budget, more innovation, and more protocol options to compensate potential pitfalls however, this revision advances a new research strategy for temperature imaging. Plan A will be to build a whole body coil for both thermal induction and thermal imaging at 3T, 7T, and for the first time at 10.5T. If indeed "things don't work out" for 10.5T, the investigators will fall back to the original plan, now Plan B of double tuning the body coil for heating at 128, 300 and 450 MHz, and imaging these temperature contours with 3T and 7T systems only. 2.) The 9.4T/65cm bore magnet, with 38 cm i.d. gradients can't be used for "whole body" imaging or heating experiments. 3.) The 10.5T magnet's "working out" is quite certain with a scheduled delivery in October 2011. Reviewer 2 (score =3) agreed with the "linear approach with four well defined milestones." His/her concerns were 1.) "potential pitfalls and alternative approaches were not described," and 2.) "power study is not in the grant (referred to some abstracts and papers)." In response, both of these criticisms result from space limitations in a 12 page proposal. While apologizing for the inconvenience, published material is referenced where possible. However, a brief power study description and more potential pitfalls and alternatives are included in this revision. Reviewer 3 (score = 2) says, "aims are complimentary with clear deliverables" and that the "plan...is reasonable." The concerns were: 1.) "link between the initial project and this project is missing," and 2.) The whole body coil will be limited to head testing only. The investigators hope that the "link" between the head studies done in the previous grant and the body studies planned with a body coil is clearer in this revision. Finally, Reviewer 4 (score = 4) also agrees that "the path to carrying out program is clear". The concerns were related to detail missing for, 1.) "specific computational approaches (packages)" , 2.) detailed plan to implement program, 3.) difficulties and possible alternatives, and 4.) two-compartment heat models. These points are now specifically addressed in the revision. While it is difficult to anticipate all new questions that may arise and even more challenging to answer them with sufficient detail in a twelve page proposal, it is hoped that confidence in the investigators will weigh in the balance for a favorable review.

A. Specific Aims

Engineers and scientists, those most often charged with assuring patient safety in MRI, agree that current safety practices are based more on simplified models, educated guesses, conservative guidelines and "experience," than on hard data and complete understanding. The MR industry for example focuses on predicting safety by SAR calculations from static cartoon models of human anatomy. It's well understood however that thermogenic pain, damage and stress to cells, tissues and systems are consequences of excessive temperature and not of SAR by itself. SAR is but one of six or more parameters of bioheat equations that must be solved to determine temperature. SAR alone completely ignores the thermodynamics and the physiology of the safety concern. In summary, SAR is relied upon as the safety metric of our industry not because it accurately predicts or measures human safety, but because the more difficult problems of accurately and precisely predicting and measuring absolute temperature in the human body have not been solved. Until the MRI field adapts "temperature" as its safety metric, patients are not as safe, imaging protocols are often compromised, and the "mission" embodied in this proposal is not accomplished.

The overall objective of this proposal therefore is to investigate high frequency RF heating to improve RF safety for high field MRI. Safety will be better assured by developing the means to accurately predict and measure RF temperature contours in human anatomy. Through development of new theory, technology, methodology, and experimental approach, these means will be achieved by accomplishing the following aims. First, a more fundamental understanding of the electrodynamics and thermodynamic nature of RF induced heating and heat transfer in anatomy will be furthered through mechanistic improvement of the empirical Pennes Bioheat Equation. Second, this new theoretical model will be validated at high field Larmor frequencies by invasive, direct measurement of RF heating in anesthetized porcine models, by fluoroptic thermometry. The porcine model is required as an intermediate step toward understanding and measuring RF heating in humans. Toward this end, the third aim is to develop a noninvasive NMR thermometer that is accurately and precisely calibrated by the invasive fluoroptic measurement. Once confidence is gained in predicting and noninvasively measuring temperatures in pigs, these methods will be applied or correlated to monitoring RF heating in humans and so accomplishing the final aim of this study. With new understanding, data, and thermal measurement methods, high field human MRI will become safer. This proposal extends our previous work of studying safety in the head to studying safety in the whole-body during ultra-high field MRI.

Aim 1. Develop a theoretical model for thermal contour prediction in the body

The new bioheat transfer model developed for predicting head temperatures in the parent grant will be extended to thermal contour predictions for the body by deriving and incorporating new blood and tissue specific heat transfer coefficients. By this new bioheat model, temperature contours will be calculated from SAR and other parameters to identify the FDA guideline limits of 1, 2, and 3 °C above core temperatures in the head, trunk, and limbs respectively.

Aim 2. Develop a porcine model for thermal contour measurement and validation

FDA guideline temperature limits will be identified in human-adult-sized, anesthetized porcine models. These temperature measurements vs. time will be made at 128, 300, and 450 MHz for 2 and 4 W/kg SAR in the porcine body. These measurements will also be used to validate and refine the theoretical predictions of Aim 1 and MR temperature measurements of Aim 3.

Aim 3. Develop MR thermometry for noninvasive / minimally invasive thermal imaging in porcine model

A new motion corrected proton resonance frequency (PRF) shift based MR thermometry method will be developed for noninvasive MR temperature measurements with the goal of 0.2 °C accuracy and precision. These temperatures will be compared to the temperatures acquired by a second chemical shift imaging method using the exogenous reagent $TmDOTA^-$ to achieve 100 times greater sensitivity. These MR thermometry methods will be calibrated and validated with fluoroptic measurements in porcine models by Aim 2 and will further validate predictions of Aim 1.

Aim 4. Predict and image temperature contours in humans

With confidence gained in the theoretical model and MR thermometry methods, temperature contours will be predicted and monitored in human bodies to assure that the FDA guidelines are not exceeded for the power settings, frequencies, and scan times studied. Well characterized methods and data for accurately predicting and noninvasively monitoring RF safety in ultra-high field human MRI will be achieved.

B. Research Strategy

B.1. Significance RF heating in ultra-high field MRI is not well understood (1). The consequences of not knowing the temperature induced by an RF excitation protocol in a human body are two-fold. 1.) Human safety is based on a "guess". 2.) A "safe" guess necessarily requires use of overly conservative, low-performance pulse protocols. A better understanding of RF heating will make high-field MRI significantly safer and more powerful, which is the objective of this study.

B.1.1 The RF Safety Problem Described A significant problem is that modern high-field MRI systems and practices rely on predicting and monitoring SAR for safety compliance (2-8). This approach is problematic however, being both protocol limiting and potentially dangerous. The SAR approach to RF safety is taken presumably because RF power input into a coil is easy to measure. At lower field strengths (<1.5T) and longer Larmor wavelengths (> 50 cm in tissue), SAR distribution over a body is more uniform. Average SAR input in units of average watts per kilogram is easy to conceptualize. SAR's effect on heating is more uniform. At these lower fields, less SAR is expended to make an image by a standard pulse sequence; there is less tissue loss and therefore less heating. "Being conservative" with RF power use is "good enough" for safe and successful MRI. Problems arise with this "averaged SAR" approach as we advance MRI to higher fields in search of higher SNR and other benefits. As the Larmor wavelengths in high-water content tissue decrease to 28 cm, 12 cm, and 8 cm for 3T, 7T, and 10.5T respectively, RF excitation wavelengths become significantly smaller than anatomic dimensions, leading to highly nonuniform B_1 and E fields over the body. When this excitation signal comes from multiple coil element sources as with a body coil, interference patterns further degrade RF field uniformity into highly localized patterns of excitation B_1 field, SAR, and temperature. Note that these local patterns of B_1, SAR, and T do not spatially correlate. See Figure 1. As RF ohmic and dielectric tissue losses increase in respective direct and quadratic proportion to frequency, SAR increases as well. To acquire a given image, more power is needed and more SAR and heating result. The need therefore to better understand, predict, and measure this heating becomes critical to the effectiveness of the MR application, and most importantly to the safety of the human patient or research subject. It is equally important to understand that temperature T and not SAR is the source of sensation (pain), thermogenic cellular damage (burns) and systemic stress (heat stroke). Measuring SAR accounts for the electrodynamics only and not the thermodynamics or thermoregulatory response of the living system under study. SAR is but one of six important parameters necessary to calculate temperature in the bioheat equations, and by itself an inadequate predictor or indicator of safety. We therefore must find ways (as in this proposal) to predict and measure in vivo temperature with sufficient accuracy and precision (0.2 °C) to facilitate careful protocol planning and safety assurance. At higher fields the safety margins are too close to continue practicing safety by the current conventions.

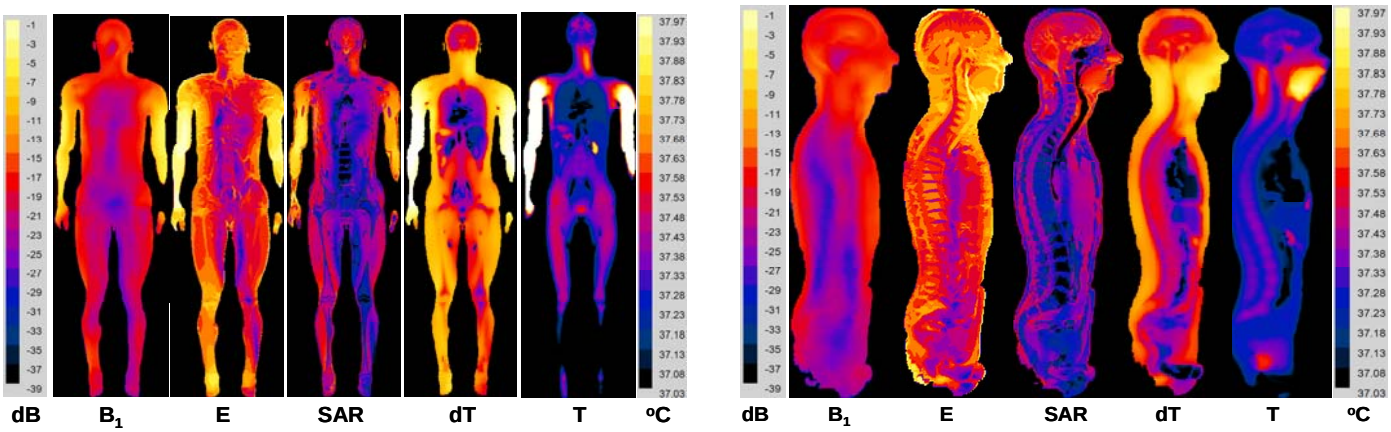

Figure 1. Calculated relative RF magnetic field (B_1), RF electric field (E),specific absorption rate (SAR), temperature change (dT), all on log scale (dB), and absolute temperature (T, °C) for 133 W, 300 MHz RF input into a 72 kg human body from a 60 cm i.d, 1 m long TEM body coil with 33cm elements centered on the thorax.

B.1.2 The RF Safety Problem Illustrated Figure 1 above makes use of preliminary results to illustrate the importance and complexity of the problem at hand. Coronal and sagittal views of the whole body inside a transmitting body coil within the shielded magnet bore are shown. SEMCAD (SPEAG, Zurich) finite difference time domain methods were used to numerically solve electrodynamic and thermodynamic contours important to the understanding of RF propagation, loss, and consequential heating in the body at ultra-high frequencies.

Four conclusions can be drawn from Figure 1 that illustrate the importance and complexity of predicting and measuring induced heating in high-field MRI. First, as expected SAR shows a highly non-uniform distribution, concentrated primarily in the arms and the peripheral tissues located close to the coil elements. However, it is counter-intuitive why tissues well outside of the body coil's elements have increased SAR levels; this can be seen in the legs and especially in the head and brain. This underscores an important understanding that SAR must be considered for the whole body and not simply the trunk within the active elements (FOV) of the array. Second, the heating increase (dT) does not always spatially correlate to SAR. In Figure 1 the heating increase correlates approximately spatially with the SAR distribution everywhere, except in the brain. The well-perfused brain is cooler than SAR contours alone would predict. Third, the absolute temperature magnitude, T, is more important than the heating change, dT. Note the heating change contours predicting hot arms, shoulders, and neck. However the absolute temperature shows additionally increased temperatures in the lower pelvis and a single kidney. Fourth and finally, SAR does not adequately predict the absolute temperature. In the Figure 1 example, RF energy is input at 1.8 W/kg, well under the 4 W/kg SAR guideline limit for the body. However the arms and shoulders, neck and a kidney have reached or exceeded the guideline temperature limit in the head and body (1, 9). The temperature calculated above by Pennes Bioheat equation will be improved by including dynamic temporal and spatial blood temperature in a new model proposed herein. The models of Figure 1 clearly demonstrate that the imaging volume (B_1), SAR, temperature change (dT), and absolute temperature magnitude (T) are independent parameters. None can be substituted for, or used alone to predict temperature T, apart from their relationships through the bioheat equations.

B.1.3 RF Safety Research Needed. In addition to the general need for understanding, predicting, and measuring high field MRI induced heating as described above, a number of practical needs are pressing for these solutions as well. While human patients and healthy subjects are being imaged at 3T - 9.4T and soon 10.5T, RF heating data in vivo at these ultra-high fields are scarce to nonexistent (10-19). No RF heating data in vivo is found in the literature for whole body imaging at 3T and above. This is alarming considering that there are more than two thousand 3T clinical systems and nearly forty 7T research systems. All 3T and 7T systems in use today have FDA and IRB clearances respectively, based primarily on SAR models as shown in Figure 1. Meanwhile, the University of Minnesota is installing a 10.5T MRI system for whole body imaging. This system represents a significant investment and show of support from the NIH and from the State of Minnesota. No human studies may be performed in that system until many of the models and measurements proposed herein are performed and approved by the FDA, IDE process, and our own IRB. While conservative RF pulse protocol management, lower radio frequencies and experience are to be credited for its strong safety record, MRI is not practiced without incident. The manufacturer and user facility device experience (MAUDE) database of the US Food and Drug Administration (FDA) records ~464 adverse events related to MRI since 1992. Most of these events are related to RF heating and are associated with MR scanners of ≤ 3T static field strength. There is an annual increase in RF heating related MRI accidents of about 30% since 2004 until 2009. Given the voluntary nature of the reporting and the number of annual MR scans the FDA expects the actual number of incidences to be four times larger than reported. The adverse events have prevented the FDA from raising SAR limits. RF heating is expected to be worse and less uniform in the new higher field systems. The work of this proposal is called for.

RF safety research is needed for clinical and research subjects. Arguments as to whether this work has clinical relevance or whether it is innovative truly should not apply where human safety is at stake. Thousands of humans are now being imaged annually at ultrahigh fields (UHF). Because human subjects might not (yet) be imaged for "clinical" purposes at 7T or 10.5T does not make "research" imaging more safe or less important. And whether or not imaging the whole body at 7T or 10.5T for the first time is considered clinical or innovative, high field imaging is less safe without this or similar work to predict, measure, understand, and establish the RF dosimetry boundaries. Further, 3T is a clinical field strength. The proposed research is unique for investigating RF safety in theory, in live porcine models and in humans at ultra-high field strengths. Until the RF safety questions are answered, the problems are solved and people are safe, this work needs to continue.

B.1.4. Industry Advocacy for RF Safety Research. The investigators submitting this proposal are not alone in realizing the significance and need for the proposed research. The major international industry regulatory groups: International Commission on Non-Ionizing Radiation Protection (ICNIRP) and the International Electrotechnical Commission (IEC) are calling for this research. According to ICNIRP “further investigation to define more precisely the spatial deposition of RF energy during an MR procedure and the corresponding

temperature fields in the human body using a three dimensional bioheat transfer model is needed"(1). Dr. Joe Schaefer's (GE Senior Scientist) letter from the IEC is attached. Additional letters attached from Siemens and Philips of the MR industry also advocate for the proposed work.

B.2. Innovation The proposed research challenges current research and clinical practice paradigms because it addresses head-on the important problem of RF heating in humans during imaging in ultra-high field MR scanners (3T, 7T, and 10.5T). This research seeks to shift current research and clinical practice paradigms because it has definite, careful, and achievable goals to perform RF safe, whole-body MR imaging. Innovations to be developed are summarized below.

B.2.1. A Validated Theoretical Bioheat Transfer Model (Aim 1) The generic bioheat transfer model (GBHTM) derived previously (20) and adapted to predict head temperatures will be extended to predict RF heating in the body by developing new blood-tissue heat transfer coefficients. The new model will help to better understand and predict the RF energy thermal transport and RF heating in the whole body anatomy during UHF MRI. No such validated bioheat model is available.

B.2.2. RF Heating Data Acquisition (Aims 2) New methods, technology, and field strengths will be developed and used to acquire unique heating data from porcine models. In vivo RF heating data will be acquired from human adult sized, anesthetized pigs at the Larmor frequencies of 128 MHz (3T), 300 MHz (7T) and 450 MHz (10.5T). This RF heating data will be acquired with a 16 channel, TEM body coil tuned to each of these respective frequencies and used for both heating and thermal image acquisition. See Figure 2. This image data will be calibrated with direct fluroptic temperature vs. time measurements. The resulting thermal imaging data will give immediate and useful insights into RF heating at the highest fields and will be used to validate the new bioheat model and MR thermometry methods developed. The coil is described further in section B.3.2.3.

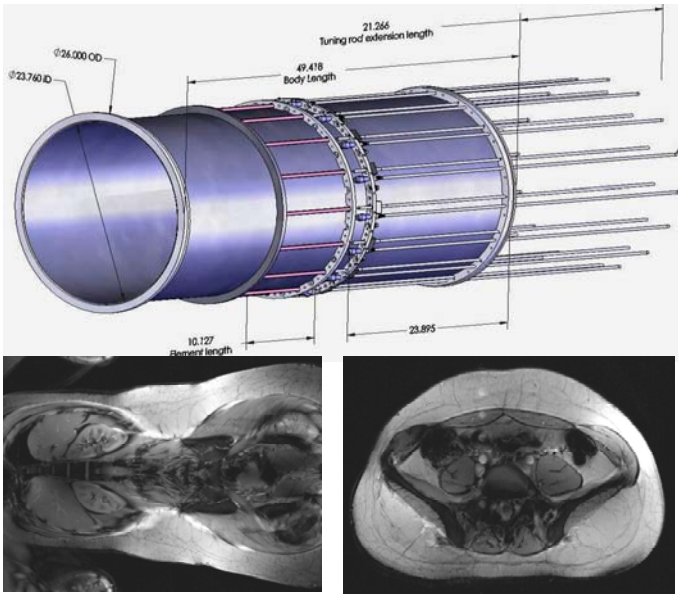

Figure 2. 16 channel transmit body coil (above) and first 7T whole body images thereby acquired (below).

B.2.3. A Validated MR Thermometry Method (Aim 3) A novel, motion corrected proton resonance frequency shift (PRF) based MR thermometry method will be developed to image RF heating with an accuracy of ≤ 0.3 °C in swine and humans with the help of our consultant Dr. Kim Butts Pauly. Dr. Butts Pauly is an expert in developing motion corrected PRF based thermometry techniques (21-26). In addition to optimizing and validating the PRF based MR thermometry method, for porcine models we will explore the application of novel MR thermometry techniques based on the strong temperature dependence of hyperfine shifted proton signals from paramagnetic lanthanide complexes. Our consultant/collaborator, Dr. Navin Bansal, has shown in many publications that the chemical shifts of Tm-based macrocyclic complexes, such as $TmDOTA^-$, are 100 times more sensitive to temperature than water proton frequency shifts (27-32). The feasibility of imaging absolute temperature with a paramagnetic lanthanide complex using water as a reference has been demonstrated in rodents (30). The proposed research will extend this TmDOTA based MR thermometry to the porcine model.

B.2.4. Ultra-high Field MRI of Humans and RF Heating Data In Vivo (Aim 4) RF safe whole-body MR imaging will be achieved in 3T, 7T, and 10.5T at the maximum allowable whole-body average SAR. Temperatures in the body will be predicted using the validated bioheat model and imaged using the validated MR thermometry method to keep the maximum temperature change below a set threshold.

B.3. Approach RF safety in high field human MRI will be better ensured by developing the means to accurately predict and measure RF heating in human anatomy. More specifically; 1.) a theoretical bioheat transfer model will be developed to understand thermal transport and predict RF heating (Aim 1); 2.) direct fluoroptic measurements of RF heating will be made in human-adult-sized swine to validate the theoretical model of Aim 1 and MR thermometry methods of Aim 3 (Aim 2); 3.) PRF and $TmDOTA^-$ based fast and accurate MR thermometry methods will be developed to image RF heating (Aim 3); and 4.) RF safe MR

imaging will be achieved in humans in 3T, 7T, and 10.5T at the FDA allowable maximum whole-body average SAR of 4 W/kg (Aim 4) – the ultimate goal of the study. Presented below are plans to achieve our aims.

B.3.1. Derive A Theoretical Bioheat Transfer Model to Predict RF Heating (Aim 1) A theoretically rigorous, bioheat model will be developed to predict RF heating in the body. To achieve this aim, the following five tasks will be completed: 1.) derive first principles based bioheat model; 2.) determine blood-tissue heat transfer coefficient to determine thermal energy interaction between the blood and the surrounding tissue; 3.) segment porcine body, and assign electromagnetic and thermodynamic properties; 4.) obtain RF power distribution by solving Maxwell's electromagnetic equations; 5.) calculate RF heating by solving the new bioheat equation. Our ability to accomplish the above tasks is presented below in sections B.3.1.1 – B.3.1.5.

B.3.1.1. Derive a Theoretical Bioheat Transfer Model for Ultra-high Fields A new, theoretical bioheat model, the Generic Bioheat Transfer Model (GBHTM) has been derived from first principles to predict temperature distribution in a perfused, heated tissue (Equation 1)(20) as part of our parent grant. The theoretical model provided explicit relationship between the mathematical model parameters and physiology. Enhanced theoretical understanding between the model parameters and the underlying physiology resulted in significantly improved RF heating predictions when compared to the gold standard, the Pennes empirical bioheat transfer equation, a one compartment bioheat model (10, 20, 33) (section B.3.1.5, Figure 5).

$$(\rho C_p)\frac{\partial T_T}{\partial t} = \nabla.k\nabla T_T + \frac{<(US)_{Bl-T}>}{1-\varepsilon}(T_{Bl} - T_T) + Q_T \quad [1a]$$

$$(\rho C_p)\frac{\partial T_{Bl}}{\partial t} = \nabla.(PC_pT_{Bl}) + \frac{<(US)_{Bl-T}>}{\varepsilon}(T_T - T_{Bl}) + Q_{Bl} \quad [1b]$$

Where, ρ (density, kg.m^{-3}), C_p (specific heat, J·(kg·K)$^{-1}$), T (tissue temperature, K), t (time, s), k (thermal conductivity, W·(m·K)$^{-1}$), $<(US)_{Bl-T}>$ (blood-tissue heat transfer rate coefficient, W·K^{-1}m^{-3}), ε (blood volume fraction), Q (source term, W·m^{-3}), subscript T(tissue) and Bl (blood).

The GBHTM requires as inputs thermal properties ρ, C_p, and k, blood-tissue heat transfer coefficient $<(US)_{Bl-T}>$, and the RF power distribution. Thermal properties of various tissue types are widely studied and available in literature (34). The GBHTM was adapted to predict accurate head temperatures by optimizing the blood-tissue heat transfer coefficient parameter in our parent grant. The GBHTM will be extended by developing new values for the heat transfer coefficient to predict heating in the body. The new bioheat model will be solved in segmented swine and human models. The GBHTM predictions will help design MR protocols such that to keep maximum temperatures below the IEC guidelines for the RF power levels, frequencies, and scan times studied in both, swine and humans.

B.3.1.2. Quantification of the Blood-Tissue Heat Transfer Coefficient ($<US_{Bl-T}>$) A new blood-tissue heat transfer coefficient will be determined using first principles by considering non-linear temperature variations along thermally important vessels in heated tissue. These derivations will extend our previous derivations which assumed linear temperature variation along the vessels (35-42). *Pitfalls and Solutions* In case these new heat transfer coefficients fail to predict accurate temperatures, an optimum value of the coefficient will be obtained by minimizing the error between the predicted and fluoroptic temperatures (more in section B.3.2.8)

B.3.1.3.Tissue Segmentation A whole-body pig model will be developed by segmenting different tissue types and assigning appropriate electromagnetic and thermal properties to those tissues from high resolution (e.g., ~1 mm isotropic) whole-body images of a ~70 kg pig. One pig will used in year 1 for this purpose. The segmented pig model will be used to facilitate the experimental validation of the new bioheat model. Next, a relatively more time efficient five-tissue (i.e., skin, muscle, fat, bone, and air) whole-body pig model will be developed and evaluated to determine the feasibility of developing a similar whole-body human model to compute subject-specific RF heating. Subject-specific whole-body human models (to be developed in-house)

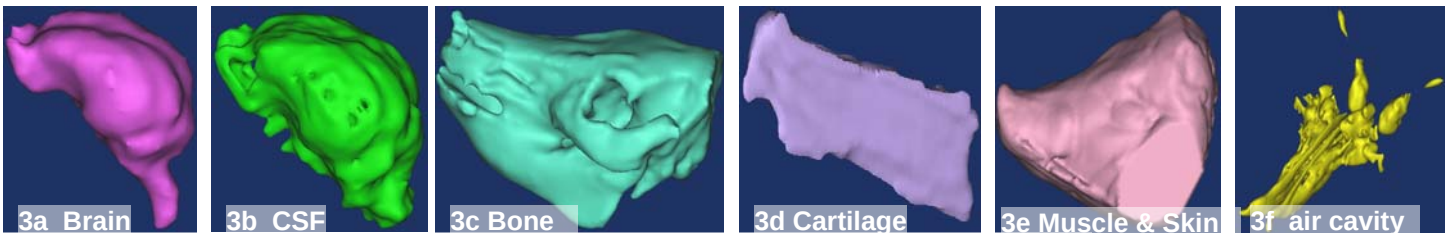

Figure 3. A segmented porcine head model developed for the parent grant.

and commercially available, segmented whole-body human models of various sizes will be used to study RF heating in the human body. All segmented porcine and human models, and other appropriate numerical codes will be made available on our website for their future use by other researchers. Our models will also be made available to industry partners (see Siemens letters) and to the regulatory industry. Figure 3 shows a segmented porcine head developed in-house as an example of our ability to develop a segmented body model (43).

B.3.1.4. Determining RF Power Distribution (Q_{RF}) RF power distribution as power loss density will be solved numerically for the coil-body model using commercial XFDTD packages and the in-house segmented whole-body models. Commercial packages used are from SEMCAD,SPEAG, Zurich,CH, and REMCOM, State College, PA. The power loss density contours will be equated to temperature by the new bioheat model, coded in-house using MATLAB and C, to determine RF heating for various coil configurations and excitation protocols. The effect of the numerical accuracy in the SAR calculation at tissue boundaries on the simulated temperatures will be studied. This error in temperature calculations is expected to be within physiological variability due to the dominating roles of blood flow and thermal diffusion. Modeled and measured In vivo temperatures matched closely in our previous whole-head heating experiments (see Figure 5 below) (10, 17).

Figure 4 shows RF power distribution in a segmented model of a pig atlas created in house for this study. The power distribution was obtained in the segmented porcine head model shown. A transmit and receive 9.4T volume head coil was used. In **Figure 4a**, a pig head was imaged in three dimensions. In **Figure 4b** the anatomy was segmented, assigned respective permittivity and conductivity for the anatomic segments, and placed inside the head coil. **Figure 4c** shows electromagnetic (EM) field and SAR calculations from this model in each of three center slice dimensions at 400 MHz.

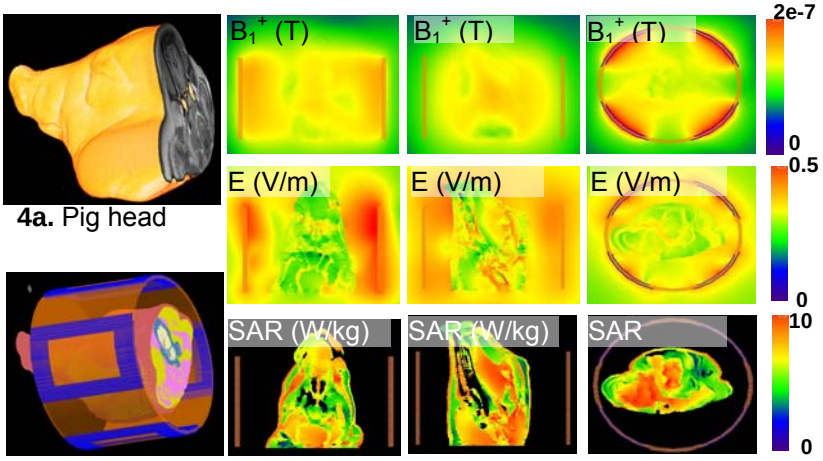

4a. Pig head

4b. Head in coil **4c.** EM field and SAR calculations

B.3.1.5. Predicting RF Heating

RF power induced temperature changes will be predicted by solving the GBHTM in the segmented whole-body models for various RF power levels, coil configurations, and excitation protocols. The predictions will facilitate better understanding of the RF heating at the highest fields and the design of RF safe MR scanning protocols to keep the maximum temperatures below set thresholds.

Figure 5 shows validation and implementation of our GBHTM. The figure shows RF heating predictions of the GBHTM in the porcine brain against the fluoroptic measurements in four ~110 kg swine. The heating was produced with an 8 channel, 7T head coil for the whole head average SAR of 3 W/kg. The mean of the experimental data (solid black line) and 95% CI are also presented (10, 11). As mentioned before, the GBHTM was derived and adapted to predict RF heating during head imaging as a part of our original RF safety grant. Extending this work, further development of the GBHTM to predict whole-body RF heating at ultra-high fields is proposed.

B.3.2. Develop an Animal Model for Thermal Contour Measurement (Aim 2) Human-adult-sized swine will be used for whole-body RF heating measurements. The measurements will be made using fluoroptic temperature probes to validate the GBHTM and MR thermometry methods. Outlined herein is the justification for using swine as an animal model (B.3.2.1), methods to produce and image RF heating (B.3.2.2), body coil used for heating and thermal imaging (B.3.2.3), fluoroptic probe placement for gold standard thermometry (B.3.2.4), justification for required animal numbers (B.3.2.5 & B.3.2.6), animal experiment plan (B.3.2.7), and the statistical analysis necessary to validate

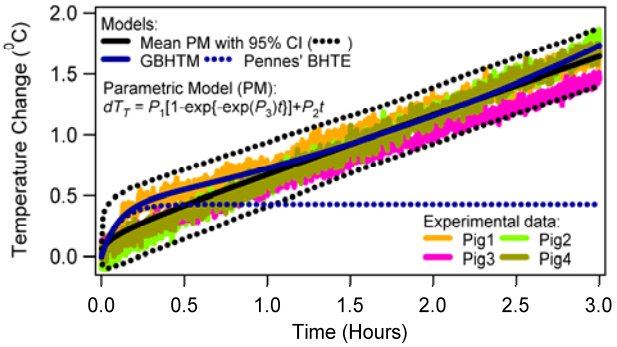

Figure 5 RF heating in the brain @7 T

the model developed in Aim 1 (B.3.2.8).

B.3.2.1. Swine as an Animal Model A pig is a thermo-physiologically similar and conservative animal model of a human. A pig has human-comparable thermal mass, surface area, water loss through skin below it's critical, hot environmental temperature, metabolic energy per unit surface area, cardiac output, electromagnetic and thermal properties, and thermoregulatory mechanisms – making it thermo-physiologically similar to a human (34, 44-47). The critical hot environmental temperature limit for a pig (36 °C for a newborn, 30 °C for a mature) is comparable to and lower than that of a human (37 °C for a newborn, 43 °C for a mature) – making it a thermo-physiologically conservative animal of a human. Human comparable thermal mass, surface area, and electromagnetic properties allow a pig to load a body coil similar to a human.

B.3.2.2. RF Heating The thermal imaging sequences will be modified to measure temperature and simultaneously provide additional prescribed SAR during heating periods so that cooling doesn't occur while imaging. In the baseline and cooling periods (the first and last 90 minute periods) minimal RF power will be used for imaging. The power that is deposited during low SAR imaging will be minimized by using minimal flip angles and sparse measurements (every 15 minutes). Power absorption due to low SAR imaging sequences will be measured. The control experiments will experience this same level of RF deposition to match the controls to the experiments. During the periods of heating, excess RF power will be added to the pulse sequence to produce/maintain heating while simultaneously measuring temperature. The sequences that measure $TmDOTA^-$ resonant frequencies will use increased flip angle and decreased TR to produce required power deposition without exceeding the Ernst angle. This will only improve the sensitivity. For the sequences to measure water PRF, additional off-resonance flip/flip-back RF pulses will increase the SAR to the prescribed levels while leaving the magnetization essentially untouched.

B.3.2.3. Body Coil In order to measure RF heating in live, anesthetized pigs and ultimately humans by NMR, a body coil will be built for imaging and heating at 3T, 7T, and for the first time ever at 10.5T. A 16 channel TEM whole-body coil will be constructed (Figure 2); each coil element will be independently tuned and matched and decoupled from neighboring elements. The methods, materials and operation of this coil are described in (48); the outer diameter of the coil will not exceed 65 cm as to fit inside the gradient coils of each magnet. Initially all 16-elements will be tuned and matched to 128 MHz (3T) for imaging and heating studies. Upon completion of the 3T studies, the array will be re-tuned to 300 MHz (7T) and 450 MHz (10.5T) and the same studies will be performed. *Pitfalls and solutions* In the event that PRF imaging at 10.5T proves unfeasible, 8 elements of the coil will be tuned to 300 MHz and the remaining 8-elements will be tuned to 450 MHz; the lower frequency elements will be used for imaging in the 7T magnet while the eight 450 MHz elements will be attached to broadband amplifiers to produce a 10.5T (450 MHz) thermal field in the subject placed in the coil. Sixteen 2 kW broadband (40-450 MHz) amplifiers purchased from CPC, Happauge, NY with Stimulus Grant S10 RR25437 will be used for imaging and heating studies (49).

B.3.2.4. Fluoroptic Temperature Probe Placement RF heating will be measured invasively using 36 fluoroptic temperature probes. The temperature probes will be placed in the head as well as trunk. In the head, the probes will be placed in the sub-cutaneous layer of the scalp, and 5 mm, 10 mm, 15 mm, 20 mm, and 25 mm deep in the brain after the dura. Probes in brain will placed in the radial direction and in one of the hemispheres through an 18 guage burr hole drilled in the skull. In the trunk, probes will be placed in three locations 25 cm apart starting from the rectal end of the pig. Nine probes will be placed in the radial direction in each of the three locations, 2 cm apart starting from the skin of the pig and ending 16 cm deep in the pig. One probe will be placed in the rectum of the animal and a second probe will be placed in the air near the animal in the coil. The room temperature and humidity will also be recorded. The PIs have extensive experience in measuring heating using fluoroptic probes (10, 11, 13-16, 50).

B.3.2.5.Sample Size (Power Study) Five 60-80 kg pigs will be used for each experimental setting to validate the bioheat model and MR thermometry methods. The sample size of 5 was determined based on the prior in vivo RF heating data in 60-100 kg swine (10, 11, 13-16). More specifically, the statistical model for pig i temperature is $y_i(t)= h_i(t)+ e_i(t)$ where $h_i(t)$ is the true temperature above core and $e_i(t)$ is probe error, averaged to be zero over windows $t \in [0, T]$ as readings are taken every second. Thermometry or bioheat prediction is $c_i(t)$, and $b_i(t) = c_i(t) - h_i(t)$ is prediction bias, the difference between theory and observed data. The model is valid if $|b_i(t)| < \Delta$ for $t \in [0, T]$. Model validity at t is checked by hypothesis $H_0: E\{ b_i(t) \} = 0$. The probability of wrongly rejecting that the model is valid is 0.05, and specify tolerance bound $\Delta = 0.05$. Prediction bias is smaller than the pig-to-pig variability, estimated at $\sigma \approx 0.02$ from prior analyses. To detect a difference of $\Delta = 0.05$ we have statistical power of 0.98 when $m = 5$. This drops to 0.62 when $m = 3$. The probability of *wrongly*

stating that the model is valid *when it is not* increases from 2% to 38% when the number of pigs are decreased from 5 to 3.

B.3.2.6. Experimental Settings and Total Number of Pigs Required RF heating is a function of the field strength (3T, 7T, 10.5T) and power deposition (i.e., whole body average specific absorption rate (SAR)) for a given coil and biological model. RF heating will be studied due to RF power deposition at 128 MHz (3T), 300 MHz(7T) and 450 MHz (10.5T) for the following three whole body average SARs: 0, 2, and 4 W/kg. Thus, a total of (5 swine per SAR level)*(3 SAR)*(3 field strengths) = 45 swine will used. Studying heating with the whole-body average SAR of 3W/kg has been removed in this revised version to minimize pig usage.

B.3.2.7. Experimental Plan Each pig will be rested for at least 6 days after its arrival to the animal facility of the CMRR to avoid anxiety and will be fasted for 12 hours before the induction of anesthesia to avoid complications (51). Water will be provided ad libitum during the fasting. For the experiment, first the animal will be immobilized and sedated using 5-10 mg/kg Telazol (Tiletamine HCl + Zolzepam HCl). The animal will be weighed to calculate the RF power needed for the intended whole-body average SAR exposure. This will be followed by intubation or tracheotomy. The animal will be kept anesthetized during the experiment (~8 hrs) using 2-3% isoflurane in 50%-50% air-O_2. Respiratory rate will be set to 12-13 cycles/min using a ventilator (Ohmeda 7000). Minute volume will be set between 7-8 L/min. Saline (0.9% NaCl) will provided through an ear vein at the rate of ~0.4-0.6 L/hr to keep the animal hydrated during the experiment. Next, MR Thermometry contrast $TmDOTA^-$ will be infused through the ear vein at the concentration of 1 mM/kg of animal weight. Nephrectomy will be performed to reduce clearance of the $TmDOTA^-$. Afterwards, fluoroptic temperature probes will be placed at pre-determined locations and depths. Temperatures will be recorded for 90 minutes before the deposition of RF power (pre-RF epoch), for 90 minutes during the RF power deposition (RF epoch), and for 90 minutes after the termination of the RF power (post-RF epoch). Net, RF power (forward minus reverse) delivered to the body coil will be measured before the coil using a power meter. At the end of the experiment, the animal will be euthanized using a saturated KCl solution.

B.3.2.8. Validating the Bioheat Model and the MR Thermometry Method Temperature vs. time data curves collected using the fluoroptic temperature probes from the heating experiments will be compared to the GBHTM predictions and the MR thermometry images for statistical goodness of fit. The central hypothesis that will be tested is that the absolute temperature difference $b_i(t)$ between a prediction/temperature image $c_i(t)$ and the corresponding direct measurement $h_i(t)$, yielding $b_i(t)=c_i(t) - h_i(t)$, is within tolerance, $|b_i(t)| < \beta$, for all $t \in [0, t]$. Accepting this hypothesis indicates that there is no statistically significant difference between the predictions/temperature images and real measurements for a given experimental setting over the time window $t \in [0, t]$, *i.e.* that the model is valid. The test will be carried out via a functional data analytic approach, which reduces the test to one of basis coefficients in Fourier expansions of $b_i(t)$. *Pitfalls and Solutions* If model validity is rejected, an optimal blood-tissue heat transfer coefficient $\langle US \rangle_{Bl\text{-}T}$ parameter value and an optimum total PRF shift coefficient value will be computed via a leave-one-out cross validation approach. Specifically, data from each of the 36 probes will sequentially be removed, and the $\langle US \rangle_{Bl\text{-}T}$ and the total PRF shift coefficient parameter that best predicts the omitted data based on the remaining 35 will be calculated (52).

At the completion of this aim, we will have an experimentally validated bioheat model that can accurately predict thermal response to SAR - thus providing a useful "correlation" between SAR and safety (temperature).

B.3.3. Develop NMR Thermometry in Porcine Models, Validated by Direct Fluoroptic Measurements (Aim 3)
A motion corrected PRF shift based MR thermometry method will be developed using swine to measure RF heating. Next, chemical shift imaging using $TmDOTA^-$ will be implemented to obtain higher resolution temperature maps. The two thermal maps from alternative approaches will be compared. Both methods (the PRF and the $TmDOTA^-$ based) will be validated using gold standard fluoroptic measurements. $TmDOTA^-$ frequency shifts are 100x more sensitive to temperature shifts than water; and thus, the method is expected to provide better accuracy and sensitivity in imaging RF heating than the PRF method. However, $TmDOTA^-$ (which has a similar molecular structure to $GdDOTA^-$) will only be used in swine since it is not yet approved for human use. The new PRF thermometry will be used to image RF heating in humans. Section B.3.3.1 presents plan to develop PRF shift based MR thermometry. Section B.3.3.2. presents temperature accuracy maps in two head slices obtained using a gradient recalled echo sequence PRF. Motion in the body is expected to deteriorate the temperature accuracy maps. Therefore, section B.3.3.3. presents a plan to improve accuracy by reducing motion induced artifacts in body temperature imaging. Section B.3.3.4 presents plan to obtain temperature maps using $TmDOTA^-$.

B.3.3.1. Developing PRF Shift Based MR Thermometry to Image RF Heating in Swine and Humans Total PRF shift coefficient of various tissue types will be determined for imaging applications by varying their temperature uniformly in a water bath between 35 °C and 41 °C and measuring phase changes at a set temperature. The PRF shift coefficient is affected by the change with temperature in the water proton molecular shielding (-0.01 ppm/°C), susceptibility (~0.003 ppm/°C), and electrical conductivity (21, 53-56). While it has been shown that the PRF shift coefficient associated with the molecular shielding is independent of tissue type, the dependency of the PRF coefficient on the susceptibility and electrical conductivity of various tissue types needs further investigation (21, 53, 54, 57). Typically, the contribution of the change in susceptibility and electrical conductivity on the PRF coefficient is neglected in comparison to the contribution of the molecular shielding. However, these contributions (>30%) must be included in RF safety applications to improve accuracy (58, 59).

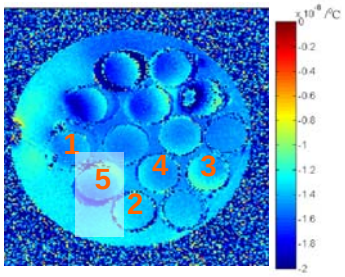

Figure 6 presents the total PRF shift coefficient map (for distilled water, a gel phantom, and various salt solutions immersed in a cylindrical water bath. The arrangement of the materials in the water bath is depicted by numbers and is as follows: 1(distilled water), and 2(1.3% agar gel, 0.9% NaCl, and 0.1mM Gd gel), 3(0.625M NaCl), 4(1.25M NaCl), and 5(2.5M NaCl). Please note that the total PRF shift coefficient is significantly different (~50%) from -0.01 ppm/°C (60). The phase drift was accounted for by using an oil sample outside the water bath.

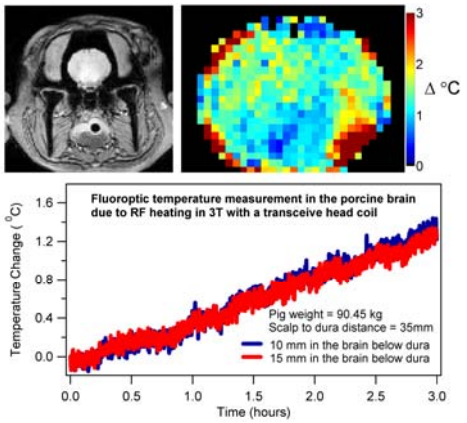

Figure 7 presents a slice of the porcine head, temperature changes imaged in the porcine brain using a total PRF shift based method, and the fluoroptically measured temperature changes in the porcine brain. Average temperature change imaged in the porcine brain after three hour long heating was 1.27 ± 0.28 °C compared to the fluoroptically measured temperature change of 1.31 ± 0.06 °C. The total PRF shift coefficient of -0.015 ppm/°C was used (59). The phase drift was accounted for by using an oil sample; more sophisticated correction techniques are proposed in B.3.3.3. to improve accuracy.

B.3.3.2. Temperature Accuracy Map with the PRF shift MR thermometry Temperature accuracy maps were obtained in the human brain with a transmit and receive head coil and a 2D GRE sequence in a 3T MR scanner (Figure 8). The maps were obtained by imaging the subject two times at a 15 minute interval without an SAR intensive scan in between. Average temperature imaging error of < 0.25 °C was achieved. Same order accuracy is expected during whole-body RF heating imaging in regions where motion and susceptibility artifacts are minimal. However, error > 2 °C is expected in regions where motion and susceptibility artifacts are significant (58, 61). The PRF thermometry will be further improved as discussed in section B.3.3.3. to image the whole body with an accuracy ≤ 0.25 °C.

RF heating due to an RF power deposition will be imaged in the swine and humans every 15 minutes. A recent report has implemented an ss-EPI sequence in 3T to measure temperature change with an accuracy ≤ 0.2 °C in the human brain (62). Depending on our needs this sequence may be modified and employed to image RF heating in humans in 3T, 7T, and 10.5T.

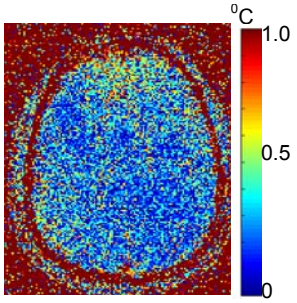

Figure 8 A typical temperature accuracy map in a live human subject. The map was obtained by imaging a subject two times at a 15 minute interval. The images were obtained with a transceive head coil and a 2D GRE sequence in a 3T MR scanner. The following sequence parameters were used: Field of view (FOV) = 215 mm x 215 mm, Resolution = 192x192, TR = 56 ms, TE = 14.8 ms, Flip angle = 25°, Averages = 3, Slice thickness = 5 mm, Total scan time = 34 s. Head motion was restricted.

B.3.3.3 Robust Imaging and Post-processing Methods for measuring Temperature-related Frequency Shifts Methods for MR thermometry, which are well established for head experiments, fail in the body mainly for the following two reasons; one, image artifacts caused by magnetic field distortions where air is trapped in the intestines; and two, artifacts related to motion due to breathing, cardiac pulsation and peristaltic movement of tissue. To tackle these problems, a novel ultrafast imaging approach based on a quasi-simultaneously acquired standard spin and a double spin-echo with EPI readout will be used as described in (62). The double

spin echo is acquired slightly asymmetric relative to the second refocusing pulse. This induces a phase shift in double spin echo, which is proportional to the frequency offset and temperature change. EPI acquisitions times have been reduced with parallel imaging combined with partial Fourier imaging to reduce EPI artifacts in body imaging (63). Larger parallel imaging reduction factors are possible at ultra-high fields to further shorten the EPI acquisition time.

The spatial resolution that can be achieved with EPI based techniques may not be sufficient for body imaging. Therefore, a segmented acquisition which is sensitive to motion will be used. To eliminate motion artifacts in segmented EPI experiments, a novel post processing method, the spectral side-band analysis (SSBA), has been demonstrated to eliminate severe imaging artifacts caused by cardiac-driven motion of the human brain stem (64). To apply this technique, a short time series of the segmented double spin echo sequence will be acquired. The SSBA will be used to separate the motion-related signal modulations from the static temperature-related phase shifts in the signal and thus, improving temperature measuring accuracy ≤ 0.25 °C.

Alternatively, the multibaseline technique can be used to estimate the background phase of repetitive motions of aqueous tissues such as the liver and brain (22, 25, 26). To do this, multiple baseline images will be acquired before heating. Then, during heating, the best fitting baseline image(s) will be used for motion correction. Once this is done, any remaining background phase can be estimated (due to drift or other field changes that are not from the repetitive motion) by estimating a low spatial frequency phase from the fat pixels. Appropriate fat and water images will be acquired for this purpose. A low spatial frequency phase function will be fit in the fat pixels to estimate this remaining phase (65). The static background phase will be compensated for in the multibaseline correction and the low spatial frequency background phase estimation will correct drift.

B.3.3.4. TmDOTA⁻ to Image RF Heating in Swine TmDOTA⁻ based in vivo temperature imaging is well established in animal systems (27-30, 32). TmDOTA⁻ will be infused through an ear vein of the pig at the concentration of 1 mM/kg of animal weight. Nephrectomy will be performed to reduce clearance of TmDOTA⁻ over time. Chemical shift imaging with the resolution of better than 2 mm X 2 mm X 2 mm will be performed using H_5 of the TmDOTA⁻. The H_5 signal of the TmDOTA⁻ is ~100 times more sensitive to temperature than the water proton signal, and is independent of the pH and calcium ion concentration (29).

The feasibility of imaging temperature of a live rat with TmDOTMA⁻ is shown in Figure 9. After injecting ~1.4 mmol kg^{-1} body-weight (bw) TmDOTMA⁻, 3D images of the methyl ^1H signal from TmDOTMA⁻ were acquired with an imaging time of ~3 min. The images have 0.94 × 0.94 mm^2 in-plane resolution, a 3.13-mm slice thickness and an SNR of 7. The TmDOTMA⁻ image in Figure 9b shows large variations in signal intensity indicating uneven distribution of the agent in the animal. This heterogeneous distribution resulted from differences in the blood flow and different fractions of extracellular space in various organs and tissue regions of the animal. However, the variation in TmDOTMA⁻ concentration does not affect temperature imaging, because the chemical shift and the temperature dependence of the chemical shift of methyl signal from TmDOTMA⁻ is independent of concentration (28), as it results from intramolecular paramagnetic interactions. The average animal temperature calculated from the 3D temperature image was 37.6 °C when the rectal temperature was 36.7 °C. Brown adipose tissue is known to generate higher temperatures than other tissues in small animals, especially when the ambient temperature is low because it has the ability to dissipate metabolic energy as heat (66).

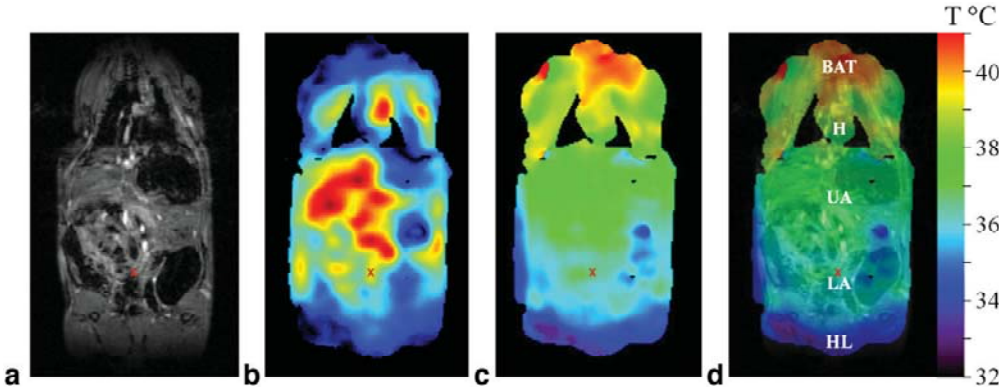

FIG. 9 Representative coronal slices of high-resolution anatomical image obtained from water ^1H signal (**a**), TmDOTMA⁻ image obtained from the ^1H methyl signal of TmDOTMA⁻ (**b**), temperature image computed from frequency of the TmDOTMA⁻ signal relative to the water signal (**c**), and the temperature image fused with the high-resolution anatomical image (**d**) showing temperature distribution in the rat in vivo. The regions of brown adipose tissue (BAT), the heart (H), the upper abdomen (UA), the lower abdomen (LA), and the hindlimbs (HL) for this respective slice showed an average temperature of 40.4, 39.1, 38.1, 36.5, and 34.4 C, respectively. The average rectal temperature (indicated by a cross-mark) was at ~36.7 C.

The macrocyclic paramagnetic lanthanide complexes, such as TmDOTA⁻ and TmDOTMA⁻ are expected to be safe for animal application at the doses necessary for MR thermometry. All the animals in the study tolerated

the injected 1.0-1.4 mmol kg^{-1} bw dose of $TmDOTMA^-$ well and did not show any acute adverse effects. Normal breathing patterns were observed before, during and after the injection of $TmDOTMA^-$. $TmDOTMA^-$, being a macrocyclic complex, is thermodynamically and kinetically more stable than the linear gadolinium complexes used as MRI contrast agents in the United States (67).

Temperature imaging experiments with the macrocyclic complex $TmDOTA^-$ will be conducted on 50 pigs (60-80 kg of body weight [bw]). The animals will be anesthetized by inhalation of 1–2% isoflurane in 100% oxygen or medical air delivered through a face mask. An ear vein will be cannulated to inject $TmDOTA^-$ during MRI experiments. The animal will be positioned on a special cradle over a pneumatic respiration sensor (SA Instruments Inc., Stony Brook, NY). 3D coronal ^1H $TmDOTA^-$ and water images will be collected before and after injecting 100 mL of 500 mM $TmDOTA^-$ solution through the ear vein catheter (0.7–1.0 mmol/kg bw). Nephrectomy will be performed to reduce clearance of $TmDOTA^-$ over time. $TmDOTA^-$ images will be acquired using GRE imaging sequence with CHESS water suppression. The following imaging parameters will be used: TR = 10 ms, TE = 1.0 ms, flip angle = 90°, adjusted for required SAR level, 128x64x16 data points zero-filled with a 60x40x40 FOV and 16 signal averages. The total imaging time for a 3D $TmDOTMA^-$ image will be 2.7 min. Water reference images will be collected using the same imaging parameters as used for $TmDOTA^-$, except a flip angle of 5° will be used and only one transient will be collected at each phase-encoding step. Pixel-by-pixel analyses of water and $TmDOTA^-$ images will be done using MATLAB (Mathworks, Natick, MA). The maps of difference in water and $TmDOTA^-$ frequencies will be calculated from the phase difference between water and $TmDOTA^-$ signals for each pixel. Temperature maps will be computed from the water and $TmDOTA^-$ frequencies using published calibration constants (30).

B.3.4. Application – Predict Temperature Contours by the Theoretical Model and Measure Temperature Contours by NMR Thermometry in Humans (Aim 4) With confidence gained in the theoretical model and NMR thermometry methods, temperature contours will be predicted and monitored in human bodies to assure that the IEC 2 ºC guideline is not exceeded for the power settings, frequencies, and scan times studied. To achieve Aim 4, section B.3.4.1. presents the overall experimental plan; section B.3.4.2. presents the justification for the sample size.

B.3.4.1. Experimental plan to achieve RF safe human head imaging RF heating will be first predicted using the GBHTM and later imaged using the PRF MR thermometry method in 15 healthy human subjects to make sure that the peak RF power induced temperature change does not exceed 2 °C in 3 T, 7T, and 10.5T with the whole body average SAR of 4 W/kg. RF power will be deposited continuously for the total duration of 45 minutes. The whole body average SAR of 4 W/kg is chosen since it is the US FDA/IEC approved maximum allowable whole body average SAR in the first level controlled mode. This value of the SAR may be adjusted to a safer, lower value based on the predictions of the new GBHM model.

B.3.4.2. Justification of the Sample Size Five healthy subjects will be used for each of the three field strengths to perform RF safe whole-body imaging. Thus a total of (5 subjects per field strength)(3 field strengths) = 15 subjects are required in the final year of the proposed study. The sample size of 5 was determined by the statistical analysis shown in Section 3.2.5. Summarizing the proposed study, the overall experimental plan is tabulated below in Table 1. Table 2 presents time line for achieving specific aims of the study.

Table 1 Plan for the yearly number of experiments

Years	Developing and validating the GBHTM (Aims 1 & 2)	Developing and validating the MR thermometry method (Aims 2 & 3)	Perform RF safe imaging in ultra-high fields (Aim 4)
1	1 pig	-	-
2	15 pigs @3T	15 pigs @3T	-
3	15 pigs @7T	15 pigs @7T	-
4	15 pigs @ 10.5T	15 pigs @ 10.5T	-
5			15 humans @ 3T, 7T, 10.5T

Table 2 Time line for achieving aims

Task	Year 1	Year 2	Year 3	Year 4	Year 5
Developing and validating the GBHTM	X	X	X	X	X
Developing and validating the MR thermometry method		X	X	X	X
Achieving RF safe MR head imaging in humans					X

Finally, this study will achieve RF safe body imaging in healthy human subjects in 3T, 7T, and 10.5T MR scanners by developing accurate and precise clinically relevant tools to understand RF energy thermal transport, and predicting and imaging RF heating. The ability to safely image the human head at the FDA guideline maximum SAR and higher SAR levels will maximize imaging protocol options. Future development and implementation of SAR-intensive sequences with shortened scanning times will be facilitated for existing and new applications with a 'safe' temperature change limit rigorously imposed.

B.3.5. Progress Report

Progress made towards the proposed specific aims of the existing RF Safety Grant (Title: NIH EB007327-01A1 – RF Safety for Ultra-High Field MRI, PI: Vaughan, JT, Beginning date: 09/15/2007, Ending date: - 06/30/2011) are summarized below. The overall objective of the grant was to investigate the RF power deposition induced heating during head imaging in ultra-high fields to improve RF safety. The RF heating was proposed to be studied at 128 MHz (3T), 300 MHz (7T), 400 MHz (9.4T), and 500 MHz(11.7T). Sections B.3.5.1.-B.3.5.4. summarize the original Specific Aims 1-4, and document their achievement. Section B.3.5.5. discusses changes made to the Specific Aims and changes resulting from significant budget reductions incurred at the onset of this project.

Progress towards the Specific Aims of the original grant has been extensive and productive, resulting in all or part of 13 journal papers, 34 peer reviewed abstracts, 4 patents, 8 invited book chapters, four edited books, encyclopedia sections and a journal special edition, and four workshops on ultra-high field MRI and Safety. See Progress Report Publication List. Additionally, 16 more peer-reviewed manuscripts (6 as journal papers in various stages of preparation, and 10 as conference abstracts/publications) are expected to be submitted by the end of the grant period. Specific progress toward the original Aims follows.

B.3.5.1. Aim 1 Develop Theoretical Model for Thermal Contour Prediction This specific aim was fully achieved. A new, three-dimensional bioheat thermal model (Generic Bioheat Thermal Model, GBHTM) was derived from first principles. The new model is the most advanced and fundamental bioheat model available for MRI.

Parameters of the new model were validated using direct fluoroptic temperature measurements in porcine heads to predict accurate RF heating during head imaging in ultra-high fields (10, 13-15, 20, 60, 68). The model was shown to improve upon the traditionally employed 'gold standard' Pennes' bioheat thermal model both theoretically and experimentally (10, 20, 60). The new model provides, for the first time, the ability to perform head imaging at the highest fields by keeping the temperatures In vivo below FDA thresholds at the allowable and potentially higher maximum whole head average SARs.

B.3.5.2. Aim 2 Develop Animal Model for Thermal Contour Measurement This specific aim is 75% complete. Direct RF heating measurements were made in porcine heads due to a CW RF power deposition with head coils at 123 MHz (3T), 300 MHz (7T), and 400 MHz (9.4T) (10, 11, 13-18, 20, 60, 68-70). These measurements are the first direct measurements of RF heating due to power deposition from ultra-high field head coils in human-adult-sized animals. These measurements provide a fundamental understanding of the underlying physics and physiology of RF heating and thus, help develop an accurate theoretical bioheat model. No measurements were performed at 500 MHz (11.74T) due to budget and time cuts. Additionally, because the 11.74T system delivery is still possibly three years away, there was no immediate and compelling need for 500 MHz heating data. However, this Aim will be completed with the new 10.5T MRI system now scheduled for delivery in October, 2011.

B.3.5.3. Aim 3 Develop NMR Thermometry in Porcine Models This specific aim is 60% complete. Total proton resonance frequency (PRF) shift coefficient has been measured ex-vivo in porcine brains for temperature imaging. Scanning protocols have been developed and optimized to image temperature changes within 90 seconds (~ thermal diffusion time constant) and with an accuracy better that ±0.25 °C (60, 71, 72). The total

PRF shift coefficient was found to be significantly different from the traditionally used molecular shielding based PRF shift coefficient of -0.01 ppm/°C. RF heating was produced and imaged at 123 MHz and 300 MHz in swine using head coils. The RF thermal imaging experiments at 400 MHz have been dropped from the Aims due to the reduction in the budget and the grant period from 5 years to 4 years. The thermal imaging experiment at 500 MHz will not be performed because the 11.7 T system at CEA Neurospin will not be operational before the end of this grant. These missed experiments however are proposed in new form for completion at 128MHz, 300 MHz, and at 450 MHz, in whole bodies in this proposal renewal. The proposed temperature measurements using the T1rho and T2rho based MR thermometry methods were attempted but abandoned in favor of a PRF shift based method since the superposition of the multiple diffusion and exchange of water protons in environments with different local magnetic susceptibilities and water-protein interactions gave non-uniform slopes (varying between positive, 0, and negative) of the T1rho and T2rho with temperature within the porcine brain, making those thermometries non-robust and un-reliable.

B.3.5.4. Aim 4 Predict and Measure Temperature Contours by NMR Thermometry in Humans This specific aim is 50% achieved. RF heating in the segmented human head models is computed using the new theoretical GBHTM method of modeling RF power deposition from ultra-high field head coils. The computations provided deeper understanding of the RF heating and facilitated better imaging plans to limit maximum in vivo temperature changes to less that the FDA RF safety thresholds. RF heating imaging in humans was dropped due to budget and time cuts. These missed experiments however are proposed in new form for completion at 128MHz, 300 MHz, and at 450 MHz, in whole bodies in this proposal renewal.

5. Progress Report Publication List

The publication productivity stemming in whole or in part from this grant is extensive in count and dimension. This reflects the importance of the "RF Safety" grant to much of the work in our laboratory, and in the MRI community. In our ultra-high field lab, hardly an investigation is attempted or a manuscript published without significant consultation, collaboration and contribution on RF Safety from the investigators of this grant. The list below, as extensive as it is, does not reflect the entirety of this grant's impact on the field. Not included for example are the FDA IDE and University IRB and IACUC documents incorporating the results of this grant. Not included are documents, collaboration and contribution to the IEC, to the European MRI+ project, to the FDA and the ISMRM Safety Working Group, ISMRM RF Heating Workshop, and the ISMRM Safety Committee, all benefitting from the results and experience gained from this grant. A reviewer of the first draft of this proposal was concerned about "padding" of these references. While the original references included publications supported by grant investigator consultation (authorship), safety regulatory documents mentioned, and by safety criteria and practices resulting from this grant, this revision has included only the publications referencing the RF Safety grant and/or including an RF Safety component and grant investigator authorship. The same reviewer had questions of overlap as well due to multiple grants being credited on many of the following references. In our lab and in others, it is common for research to be supported by more than one grant due to the scope, scale and multi-disciplinary nature of much research. This is our only grant however dedicated exclusively to supporting RF Safety and the publications below depended on it.

5.1. Peer Reviewed Journal Publications

1. Shrivastava D, Hanson T, Schlentz R, Gallagher W, Snyder C, DelaBarre L, Prakash S, Iaizzo PA, and Vaughan JT, “Radio-Frequency Heating at 9.4T (400 MHz) – In Vivo Temperature Measurement Results in Swine”, Magnetic Resonance in Medicine, 2008, Vol. 59, No. 1, pp. 73-78. PMCID: 2782895
2. Vaughan, J.T., et al., “Whole Body Imaging at 7T: Preliminary Results”, Magn Reson Med, 2009, Vol. 61: p. 244-248. PMCID: 2875945
3. Metzger GJ, Snyder C, Akgun C, Vaughan JT, Ugurbil K, Van de Moortele PF. Local B(1) (+) shimming for prostate imaging with transceiver arrays at 7T based on subject-dependent transmit phase measurements. Magn Reson Med 2008;59(2):396-409.
4. Wang, Z., et al., “Consideration of Physiological Response in Numerical Models of Temperature During MRI of the Human Head”, J Magn Reson Imag, 2008, Vol. 28, p. 1303-1308. PMCID: 2597208
5. Snyder CJ, DelaBarre L, Metzger GJ, van de Moortele PF, Akgun C, Ugurbil K, Vaughan JT. Initial results of cardiac imaging at 7 Tesla. Magn Reson Med 2009;61(3):517-524. PMCID: 2939145
6. Shrivastava D, Hanson T, Kulesa J, DelaBarre L, Gregor A, Iaizzo PA, and Vaughan JT, “Radio-Frequency Heating at 9.4T– In Vivo Thermoregulatory Temperature Response in Swine”, Magnetic Resonance in Medicine, 2009, Vol. 62, No. 4, pp. 888-895. PMCID: 2782895
7. Shrivastava D, Vaughan JT. A Generic Bioheat Transfer Thermal Model for a Perfused Tissue. Journal of Biomechanical Engineering. 2009;131(7):074506-5. PMCID: 2737815.
8. Vaughan JT, editor. Special Edition of NMR in Biomedicine: Radiofrequency Coils; Volume 22(9); 2009.
9. Shrivastava D, Abosch A, Hanson T, Gupte A, Iaizzo PA, and Vaughan JT., “Effect of Extra-Cranial Portion of a DBS Lead on Radiofrequency Heating with a 9.4 Tesla Head Coil Within Cadaveric Porcine Heads”, Journal of Magnetic Resonance Imaging, 2010, Vol. 32, pp. 600-607. PMCID:2933930
10. Wu X, Vaughan JT, Ugurbil K, Van de Moortele PF, “Parallel excitation in the human brain at 9.4 T counteracting k-space errors with RF pulse design”, Magn Reson Med 2010;63(2):524-529. NIHMS: 277138
11. Shrivastava D, Hanson T, Kulesa J, Tian J, Gregor A, and Vaughan JT, “Radiofrequency Heating in Porcine Models with a ‘Large’ 7 T (296 MHz) Head Coil”, Magnetic Resonance in Medicine, 2011, Vol. 66, No. 1, pp, 255-63 NIHMS:307590
12. Metzger GJ, van de Moortele PF, Akgun C, Snyder CJ, Moeller S, Strupp J, Andersen P, Shrivastava D, Vaughan T, Ugurbil K, Adriany G. Performance of external and internal coil configurations for prostate investigations at 7 T. Magn Reson Med. 2010;64(6):1625-39. PMCID: 2991410.
13. Snyder C, DelaBarre L, Moeller S, Akgun C, Van de Moortele P-F, Bolan P, Ugurbil K, Vaughan JT, Metzger G. Comparison Between Eight- and Sixteen-Channel TEM Transceive Arrays for Body Imaging at 7 Tesla. Magn Reson Med. 2011; in press.

5.2. Peer Reviewed Abstracts and Conference Publications

1. Shrivastava D, Hanson T, Schlentz R, Kulesa J, Gallagher W, Snyder C, DelaBarre L, Iaizzo PA, Vaughan JT, “Thermally Safe Magnetic Resonance Imaging at 9.4 Tesla and In Vivo Thermal Characterization of the Radio Frequency Head Coil”, Summer Bioengineering Conference, Colorado, USA 2007.
2. Shrivastava D, Schlentz R, Kulesa J, Gallagher W, Snyder C, DelaBarre L, Hanson T, Iaizzo PA, Vaughan JT, “Radio-Frequency Heating at 9.4T – In Vivo Porcine Studies”, ISMRM Annual Meeting, Berlin, 2007.
3. Shrivastava D, Schlentz R, Kulesa J, Gallagher W, Snyder C, DelaBarre L, Hanson T, Iaizzo PA, Vaughan JT, “MR Safety Measurements”, 6th Bi-Annual 2007 Minnesota Workshops, Minneapolis, USA, 2007.
4. Wu, X., Akgun C., Vaughan JT, Ugurbil, K., Van de Moortele, “SAR Analysis for Transmit SENSE at 7T with a Human Head Model,” ISMRM 2007.
5. Wu, X., Akgun C., Vaughan JT, Ugurbil, K., Van de Moortele, “SAR Reduction in Transmit SENSE Using Adapted Excitation k-Space Trajectories,” ISMRM 2007.
6. Tian J., Snyder CJ., Delabarre L., Akgun C., Liu W., Collins C.M., Gopinath A., and Vaughan JT., “Effect of Head Size to B1, SNR and SAR,” ISMRM 2007, Abstract 1011.
7. Bolan P, Adriany G, Akgun C, Andersen P, Auerbach E, DelaBarre L, Goerke U, Gozubuyuk A, Metzger GJ, Moeller S, Snyder AS, Snyder C, Strupp J, Van de Moortele P-F, Vaughan JT, Ugurbil K, “Technical Aspects of Ultra-High Field (7T) Body MR Imaging and Spectroscopy” Proceedings of the Radiological Society of North America, Chicago, IL (2007)
8. Shrivastava D, Schlentz R, Kulesa J, DelaBarre L, Snyder C, Hanson T, Vaughan JT, “9.4 T RF Heating – In Vivo Thermoregulatory Response in Porcine Models”, ISMRM Annual Meeting, Toronto, 2008.
9. Shrivastava D, DelaBarre L, Michaeli, Shalom, Snyder C; Hanson T, Vaughan JT, “Proton Resonance Frequency Based NMR Thermometry of Ultra-High Field RF Safety Applications”, ISMRM Annual Meeting, Toronto, 2008.
10. Shrivastava D, DelaBarre L, Hanson T, Vaughan JT, “Improved MR Thermometry to Measure Brain Temperatures”, ASME - Summer Bioengineering Conference, Marco Island, USA, 2008.
11. Shrivastava D, Kulesa J, DelaBarre L, Snyder C, Hanson T, Vaughan JT, “Identification of Possibly Unsafe RF Exposure Thresholds for Humans using Porcine Models”, ASME - Summer Bioengineering Conference, Marco Island, USA, 2008.
12. Akgun C, Snyder CJ, Moeller S, Bolan P, Vaughan JT, Ugurbil K, Van de Moortele PF, Metzger GJ Transmit and Receive FDTD Modeling as a Valuable Tool for RF Coil Development: Validation of Simulations with in Vivo Torso Imaging at 7 Tesla. Proc Intl Soc Mag Reson Med 2008;16:1196.
13. Wu X., Chang, T-H, Luo Z-Q, Akgun C., Vaughan JT, Ugurbil K., Van de Moortele, P-F, “Worst case SAR scenario as a new metric for SAR analysis in B1 phase shim,” ISMRM 2008.
14. Shrivastava D, Liimatainen, Timo, Goerke, Ute, Kulesa J, Hanson T, Michaeli, Shalom, and Vaughan JT., “Optimized Signal Intensity and T_{1r} Based NMR Thermometry for Ultra-High Field RF Safety Applications”, ISMRM Annual Meeting, Hawaii, 2009.
15. Shrivastava D, Hanson T, Kulesa J, and Vaughan JT., “RF Safety and Thermal Characteristics of Porcine Heads After Euthanasia”, ISMRM Annual Meeting, Hawaii, 2009.
16. Shrivastava D, Hanson T, Abosch, Aviva, and Vaughan JT., “RF Heating due to a Deep Brain Stimulation Electrode at 9.4 T (400.2 MHz) in Porcine Heads”, ISMRM Annual Meeting, Hawaii, 2009.
17. Shrivastava D, Hanson T, Kulesa J, Gregor, Adriany, Iaizzo, Paul, and Vaughan JT., “Thermoregulatory Temperature Response in Porcine Models due to a CW, 400 MHz, RF Heating”, Society of Thermal Medicine, Arizona, USA, 2009.
18. Akgun C, DelaBarre L, Snyder C, Tian J, Gopinath A, Ugurbil K, Vaughan JT, editors. Alternating Impedance Element for 7T Multi-Channel Transceive Coil. Proceedings 17th Scientific Meeting, International Society for Magnetic Resonance in Medicine; 2009 April; Honolulu.
19. Vaughan JT, Snyder C, Delabarre L, Tian J, Adriany G, Andersen P, Strupp J, Ugurbil K, editors. Clinical Imaging at 7T with a 16 Channel Whole Body Coil and 32 Receive Channels. Proceedings 17th Scientific Meeting, International Society for Magnetic Resonance in Medicine; 2009 April; Honolulu.
20. Vaughan JT, “7T Cardiovascular MRI”, in Society for Cardic Magnetic Resonance. 2009. Orlando.
21. Shrivastava D and Vaughan JT, “Development of an Anatomically Accurate Porcine Head Model to Study Radiofrequency Heating due to MRI”, ISMRM Annual Meeting, Stockholm, Sweden, 2010.
22. Shrivastava D, Hanson T, Kulesa J, Tian, Jinfeng, Gregor, Adriany, and Vaughan JT., “Systemic In Vivo Radiofrequency Heating in Porcine Models with a 12.5’’ Diameter, 8 Channel, 7 T (296 MHz) Head Coil”, ISMRM Annual Meeting, Stockholm, Sweden, 2010.

23. Wu X., Schmitter S., Tian J., Vaughan JT., Ugurbil, K., Van de Moortele P-F, “SAR analysis of Parallel Transmission in Cardiac Imaging at 7T,” ISMRM workshop on MR safety: RF heating of the human in MR, 2010.
24. Akgun C, DelaBarre L, Snyder C, Adriany G, Gopinath A, Ugurbil K, Vaughan JT. RF Field Profiling Through Element Design for High Field Volume Coils. 2010; Stockholm, Sweeden.
25. Akgun C, DelaBarre L, Snyder C, Sohn S-M, Adriany G, Ugurbil K, Gopinath A, Vaughan JT. Alternating Impedance Multi-Channel Transmission Line Resonators for High Field Magnetic Resonance Imaging. 2010; Anaheim, CA.
26. Tian J, Snyder C, DelaBarre L, Vaughan JT. Using Dielectrics and RF Shielding to Increase B_1^+ Efficiency and Homogeneity. 2010; Stockholm, Sweeden. p 1482.
27. Akgun C, Yoo H, DelaBarre L, Snyder C, Adriany G, Van de Moortele PF, Gopinath A, Ugurbil K, Vaughan JT. Novel 24 Element Multi-Transmit Volume Coil for High Field MRI. Proceedings 19th Scientific Meeting, ISMRM; 2011; Montreal, Quebec; 3814.
28. Akgun C, DelaBarre L, Yoo H, Snyder C, Gopinath A, Ugurbil K, Vaughan JT. Stepped Impedance Resonators for High Field MRI. Proceedings 19th Scientific Meeting, ISMRM; 2011; Montreal, Quebec; 3815.
29. Shrivastava D, Goerke U, Michaeli S, Tian J, Abosch A, Vaughan JT. An MR Thermometry-GBHTM ‘Hybrid’ Model to Determine Radiofrequency Heating near Implanted Leads in High Field Imaging. Proceedings 19th Scientific Meeting, ISMRM; 2011; Montreal, Quebec; 3767.
30. Shrivastava D, Tian J, Abosch A, Vaughan JT. Radio-Frequency Heating at Deep Brain Stimulation Lead Electrodes due to Imaging with Head Coils in 3 T and 7T. Proceedings 19th Scientific Meeting, ISMRM; 2011; Montreal, Quebec; 3764.
31. Shrivastava D, Kulesa J, Tian J, Adriany G, DelaBarre L, Vaughan JT. Radio-Frequency Heating in Swine with an 8 Channel, 7 T (296 MHz) Head Coil. Proceedings 19th Scientific Meeting, ISMRM; 2011; Montreal, Quebec; 3822.
32. Shrivastava D, Goerke U, Michaeli S, Tian J, DelaBarre L, Vaughan JT. Total Proton Resonance Frequency Shift Coefficient in the Porcine Brain to Image Radiofrequency Heating in Ultra-high Field MRI. Proceedings 19th Scientific Meeting, ISMRM; 2011; Montreal, Quebec; 497.
33. Tian J, Gopinath A, Vaughan JT. Tailoring RF Power Distribution for Body Torso MRI at 300MHz. Proceedings 19th Scientific Meeting, ISMRM; 2011; Montreal, Quebec; 3851.
34. Wu X, Schmitter S, Tian J, Vaughan JT, Ugurbil K, Van de Moortele PF. SAR Analysis of Parallel Transmission in Cardiac Imaging at 7T. Proceedings 19th Scientific Meeting, ISMRM; 2011; Montreal, Quebec; 492.

5.3. Patents

1. Vaughan JT, “RF Coil for Imaging Systems and Methods of Operation.” US Patent # 7,268,554 (Issued 9/11/07).
2. Adriany G, Van de Moortele P-F, Ritter J, Voje W, Vaughan JT, Ugurbil K; University of Minnesota, assignee. Spatially Reconfigurable Magnetic Resonance Coil. USA. 2009.
3. Olson C, Vaughan JT, Gopinath A; University of Minnesota, assignee. Radiofrequency Field Localization for Magnetic Resonance. USA. 2009.
4. Vaughan JT, Adriany G, Ugurbil K; University of Minnesota, assignee. Radio Frequency Gradient, Shim and Parallel Imaging Coil. USA. 2009.

5.4. Invited Book Chapters

1. Shrivastava D, Goerke U, Porter D, Vaughan, JT, “New Developments in Bioheat Transfer Modeling and MR Thermometry to Improve Radiofrequency Safety in High-field and Ultra-high Field MRI,” RF Safety Handbook, ISMRM publisher, 2011 (in press)
2. Shrivastava D, Vaughan JT, “Radiofrequency Heating Measurements and Models,” in Encyclopedia of Magnetic Resonance, John Wiley and Sons, 2011 (in press)
3. Shrivastava D, Vaughan JT, “Radiofrequency Heating Measurements and Models,” in RF Coil Handbook, John Wiley and Sons, 2011 (in press)
4. Vaughan JT, Shrivastava D, "RF Propagation and Loss in the Human Loaded RF Coil" RF Safety Handbook, ISMRM publisher 2011 (im press)
5. Vaughan JT. "The Parallel Transceiver for MRI" Encyclopedia of Magnetic Resonance, John Wiley and Sons, 2011(in press)

6. Vaughan JT. "The Parallel Transceiver for MRI" RF Coil Handbook, John Wiley and Sons, 2011 (in press)
7. Vaughan JT, "TEM Coils for MRI" Encyclopedia of Magnetic Resonance, John Wiley and Sons, 2011(in press)
8. Vaughan JT, "TEM Coils for MRI"RF Coils Handbook, John Wiley and Sons, 2011(in press)

5.5 Books, Encyclopedia Sections, Journal Editions

1.) RF Coil Handbook, JThomas Vaughan, John Griffiths Editors, John Wiley and Sons, 2011 (in press)
2.) Encyclopedia of Magnetic Resonance, RF Coils, J Thomas Vaughan, 2011 (in press)
3.) RF Coils for MRI, NMR in Biomedicine, Special Edition, 2010
4.) RF Safety Handbook, JThomas Vaughan, International Society for Magnetic Resonance in Medicine 2011 (in press)

5.6 Workshop Proceedings

1.) ISMRM MR Safety Workshop: "RF Heating of the Human in MRI." JT Vaughan, Chair, Devashish Shrivastava, Co-Chair, Stillwater, MN Oct 14-17, 2010.
2.) Minnesota High Field Workshop: JT Vaughan, Organizing Committee, Minneapolis, MN, Oct. 2007, 2009, 2011
3.) ISMRM High Field Workshop: "Ultra-High Field Systems and Applications: 7T & Beyond, Pitfalls and Potential" JT Vaughan, Planning Committee, Lake Louise, Alberta, Canada, Feb. 2011.

C. References

1. ICNIRP. Medical Magnetic Resonance (MR) Procedures: Protection of Patients. Health Physics. 2004;87(2):197-216.
2. van den Bergen B, van den Berg CA, Klomp DW, Lagendijk JJ. SAR and power implications of different RF shimming strategies in the pelvis for 7T MRI. J Magn Reson Imaging. 2009;30(1):194-202.
3. Collins CM, Liu W, Wang J, Gruetter R, Vaughan JT, Ugurbil K, et al. Temperature and SAR calculations for a human head within volume and surface coils at 64 and 300 MHz. J Magn Reson Imaging. 2004;19(5):650-6.
4. Prock T, Collins DJ, Leach MO. A model to assess SAR for surface coil magnetic resonance spectroscopy measurements. Phys Med Biol. 2002;47(10):1805-17.
5. Ibrahim TS, Lee R, Baertlein BA, Robitaille PM. B1 field homogeneity and SAR calculations for the birdcage coil. Phys Med Biol. 2001;46(2):609-19.
6. Collins CM, Li S, Smith MB. SAR and B1 field distributions in a heterogeneous human head model within a birdcage coil. Specific energy absorption rate. Magn Reson Med. 1998;40(6):847-56.
7. van den Bergh AJ, van den Boogert HJ, Heerschap A. Calibration of the 1H decoupling field strength and experimental evaluation of the specific RF absorption rate in 1H-decoupled human 13C-MRS. Magn Reson Med. 1998;39(4):642-6.
8. Keltner JR, Carlson JW, Roos MS, Wong ST, Wong TL, Budinger TF. Electromagnetic fields of surface coil in vivo NMR at high frequencies. Magn Reson Med. 1991;22(2):467-80.
9. CDRH-FDA. Guidance for Industry and FDA Staff - Criteria for Significant Risk Investigations of Magnetic Resonance Diagnostic Devices. 2003. p. 1-3.
10. Shrivastava D, Hanson T, Kulesa J, Tian J, Gregor A, Vaugahn JT. Radiofrequency heating in porcine models with a 'large' 32 cm internal diameter, 7T (296 MHz) head coil. Magn Reson Med. 2011;66(1):255-63.
11. Shrivastava D, Hanson T, Kulesa J, Tian J, Gregor A, Vaugahn JT, editors. Systemic radio-frequency heating in porcine models with a 12.5'' diameter, 8 channel, 7 T (296 MHz) head coil. ISMRM; 2010; ISMRM, Stockholm, Sweden.
12. Oh S, Webb AG, Neuberger T, Park B, Collins CM. Experimental and numerical assessment of MRI-induced temperature change and SAR distributions in phantoms and in vivo. Magn Reson Med. 2010;63(1):218-23.
13. Shrivastava D, Hanson T, Kulesa J, DelaBarre L, Snyder C, Vaughan JT. Radio-Frequency Heating at 9.4T– In Vivo Thermoregulatory Temperature Response in Swine. Magn Reson Med. 2009;62(4):888-95.
14. Shrivastava D, Hanson T, Schlentz R, Gallaghar W, Snyder C, Delabarre L, et al. Radiofrequency heating at 9.4T: in vivo temperature measurement results in swine. Magn Reson Med. 2008;59(1):73-8.
15. Shrivastava D, Schlentz R, Kulesa J, DelaBarre L, Snyder C, Hanson T, et al., editors. 9.4 T RF Heating – In Vivo Thermoregulatory Response in Porcine Models. ISMRM; 2008; Proceedings of the International Society of Magnetic Resonance in Medicine, Toronto, Canada.
16. Shrivastava D, Schlentz R, Kulesa J, Snyder C, DelaBarre L, Hanson T, et al., editors. RF Safety at 9.4T- Porcine In vivo Results. International Society of Magnetic Resonance in Medicine; 2007; Proceedings of the International Society of Magnetic Resonance in Medicine, Berlin, Germany.
17. Shrivastava D, Vaughan J. RF Heating In Vivo in High Field MRI. ISMRM Workshop: Ultra-high field systems and applications 7T and beyond; Lake Louis, Canada2011.
18. Shrivastava D, Kulesa J, Tian J, Adriany G, DelaBarre L, JT V. Radio-frequency Heating in Swine with an 8 Channel 7 T (296 MHz) Head Coil. ISMRM Annual Meeting; Montreal, Canada2011.
19. Boss A, Graf H, Berger A, Lauer UA, Wojtczyk H, Claussen CD, et al. Tissue warming and regulatory responses induced by radio frequency energy deposition on a whole-body 3-Tesla magnetic resonance imager. J Magn Reson Imaging. 2007;26(5):1334-9.
20. Shrivastava D, Vaughan JT. A generic bioheat transfer thermal model for a perfused tissue. J Biomech Eng. 2009;131(7):074506. PMCID: 2737815.

21. Rieke V, Butts Pauly K. MR thermometry. J Magn Reson Imaging. 2008;27(2):376-90.
22. Rieke V, Kinsey AM, Ross AB, Nau WH, Diederich CJ, Sommer G, et al. Referenceless MR thermometry for monitoring thermal ablation in the prostate. IEEE Trans Med Imaging. 2007;26(6):813-21.
23. Vigen KK, Jarrard J, Rieke V, Frisoli J, Daniel BL, Butts Pauly K. In vivo porcine liver radiofrequency ablation with simultaneous MR temperature imaging. J Magn Reson Imaging. 2006;23(4):578-84.
24. Pisani LJ, Ross AB, Diederich CJ, Nau WH, Sommer FG, Glover GH, et al. Effects of spatial and temporal resolution for MR image-guided thermal ablation of prostate with transurethral ultrasound. J Magn Reson Imaging. 2005;22(1):109-18.
25. Rieke V, Vigen KK, Sommer G, Daniel BL, Pauly JM, Butts K. Referenceless PRF shift thermometry. Magn Reson Med. 2004;51(6):1223-31.
26. Vigen KK, Daniel BL, Pauly JM, Butts K. Triggered, navigated, multi-baseline method for proton resonance frequency temperature mapping with respiratory motion. Magn Reson Med. 2003;50(5):1003-10.
27. Hekmatyar SK, Hopewell P, Pakin SK, Babsky A, Bansal N. Noninvasive MR thermometry using paramagnetic lanthanide complexes of 1,4,7,10-tetraazacyclodoecane-alpha,alpha',alpha'',alpha'''-tetramethyl-1,4,7,10-tetraacetic acid (DOTMA4-). Magn Reson Med. 2005;53(2):294-303.
28. Hekmatyar SK, Kerkhoff RM, Pakin SK, Hopewell P, Bansal N. Noninvasive thermometry using hyperfine-shifted MR signals from paramagnetic lanthanide complexes. Int J Hyperthermia. 2005;21(6):561-74.
29. Hekmatyar SK, Poptani H, Babsky A, Leeper DB, Bansal N. Non-invasive magnetic resonance thermometry using thulium-1,4,7,10-tetraazacyclododecane-1,4,7,10-tetraacetate (TmDOTA(-)). Int J Hyperthermia. 2002;18(3):165-79.
30. James JR, Gao Y, Miller MA, Babsky A, Bansal N. Absolute temperature MR imaging with thulium 1,4,7,10-tetraazacyclododecane-1,4,7,10-tetramethyl-1,4,7,10-tetraacetic acid (TmDOTMA-). Magn Reson Med. 2009;62(2):550-6.
31. James JR, Gao Y, Soon VC, Topper SM, Babsky A, Bansal N. Controlled radio-frequency hyperthermia using an MR scanner and simultaneous monitoring of temperature and therapy response by (1)H, (23)Na and (31)P magnetic resonance spectroscopy in subcutaneously implanted 9L-gliosarcoma. Int J Hyperthermia. 2010;26(1):79-90.
32. Pakin SK, Hekmatyar SK, Hopewell P, Babsky A, Bansal N. Non-invasive temperature imaging with thulium 1,4,7,10-tetraazacyclododecane-1,4,7,10-tetramethyl-1,4,7,10-tetraacetic acid (TmDOTMA-). NMR Biomed. 2006;19(1):116-24.
33. Pennes HH. Analysis of tissue and arterial blood temperatures in the resting human forearm. 1948. J Appl Physiol. 1998;85(1):5-34.
34. Holmes KR. Thermal Conductivity of Selected Tissues. In: Diller KR, editor. Biotransport - Heat and Mass Transfer in Living Systems. New York: The New York Academy of Sciences; 1998. p. 18-9.
35. Shrivastava D, Roemer RB. An analytical study of 'Poisson conduction shape factors' for two thermally significant vessels in a finite, heated tissue. Phys Med Biol. 2005;50(15):3627-41.
36. Shrivastava D, Roemer R, McKay B. An analytical study of heat transfer in finite tissue with two blood vessels and uniform dirichlet boundary conditions. Journal of Heat Transfer. 2005;127(2):179-88.
37. Shrivastava D, Roemer R. An analytical study of heat transfer in a finite tissue region with two blood vessels and general Dirichlet boundary conditions. International Journal of Heat and Mass Transfer. 2005;48(19-20):4090-102.
38. Shrivastava D, Roemer R, editors. 'Poisson conduction shape factors' for 'mixed case' counter-current heat transfer applications. Advances in Bioengineering; 2004.
39. Shrivastava D, Roemer R. An analytical derivation of source term dependent, 2-D 'generalized Poisson conduction shape factors'. International Journal of Heat and Mass Transfer. 2004;47(19-20):4293-300.
40. Shrivastava D, Roemer R, editors. A comparison between 2-D and 3-D conduction shape factors. ASME Summer Heat Transfer Conference; 2003.

41. Shrivastava D, Roemer R, editors. An analytical derivation of 2-D conduction shape factors. ASME Summer Heat Transfer Conference; 2003.
42. Cousins AK. On the Nusselt number in heat transfer between multiple parallel blood vessels. J Biomech Eng. 1997;119(1):127-9.
43. Shrivastava D, Vaugahn JT, editors. Development of an Anatomically Accurate Porcine Head Model to Study Radiofrequency Heating due to MRI. ISMRM; 2010; ISMRM, Stockholm, Sweden.
44. Mount LE. Adaptation to thermal environment - Man and his productive animals. Barrington EJW, Willis AJ, Sleigh MA, editors. Baltimore: University Park Press; 1979.
45. Duck F. Physical Properties of Tissue. London: Academic Press; 1990.
46. Gabriel C, Gabriel S, Corthout E. The dielectric properties of biological tissues: I. Literature survey. Phys Med Biol. 1996;41(11):2231-49.
47. Dewhirst MW, Viglianti BL, Lora-Michiels M, Hanson M, Hoopes PJ. Basic principles of thermal dosimetry and thermal thresholds for tissue damage from hyperthermia. Int J Hyperthermia. 2003;19(3):267-94.
48. Vaughan JT, Snyder CJ, DelaBarre LJ, Bolan PJ, Tian J, Bolinger L, et al. Whole-body imaging at 7T: preliminary results. Magn Reson Med. 2009;61(1):244-8.
49. Myer DP. Amplifier System Powers Whole-Body MRI Scans. Microwaves and RF. 2011;50(3):98-104.
50. Shrivastava D, Hanson T, Kulesa J, Vaughan JT, editors. RF safety and thermal characteristics of porcine heads after euthanesia. ISMRM; 2009; Hawai, Honolulu.
51. Becker BA, Niwano Y, Johnson HD. Physiologic and immune responses associated with 48-hour fast of pigs. Lab Anim Sci. 1992;42(1):51-3.
52. Geisser S. Predictive Inference. 1 ed. New York: Chapman and Hall.; 1993.
53. Peters RD, Henkelman RM. Proton-resonance frequency shift MR thermometry is affected by changes in the electrical conductivity of tissue. Magn Reson Med. 2000;43(1):62-71.
54. Peters RD, Hinks RS, Henkelman RM. Heat-source orientation and geometry dependence in proton-resonance frequency shift magnetic resonance thermometry. Magn Reson Med. 1999;41(5):909-18.
55. Schenck JF. The role of magnetic susceptibility in magnetic resonance imaging: MRI magnetic compatibility of the first and second kinds. Med Phys. 1996;23(6):815-50.
56. De Poorter J. Noninvasive MRI thermometry with the proton resonance frequency method: study of susceptibility effects. Magn Reson Med. 1995;34(3):359-67.
57. Peters RD, Hinks RS, Henkelman RM. Ex vivo tissue-type independence in proton-resonance frequency shift MR thermometry. Magn Reson Med. 1998;40(3):454-9.
58. Sprinkhuizen SM, Konings MK, van der Bom MJ, Viergever MA, Bakker CJ, Bartels LW. Temperature-induced tissue susceptibility changes lead to significant temperature errors in PRFS-based MR thermometry during thermal interventions. Magn Reson Med.64(5):1360-72.
59. Weis J, Covaciu L, Rubertsson S, Allers M, Lunderquist A, Ahlstrom H. Noninvasive monitoring of brain temperature during mild hypothermia. Magn Reson Imaging. 2009;27(7):923-32.
60. Shrivastava D, Goerke U, Porter D, Vaughan J, editors. New developments in bioheat transfer modeling and MR thermometry to improve radiofrequency safety in high field and ultra-high field MRI. ISMRM - RF Safety Workshop; 2010; ISMRM - RF Safety Workshop, Stillwater, MN.
61. de Senneville BD, Roujol S, Moonen C, Ries M. Motion correction in MR thermometry of abdominal organs: A comparison of the referenceless vs. the multibaseline approach. Magn Reson Med.64(5):1373-81.
62. Kickhefel A, Roland J, Weiss C, Schick F. Accuracy of real-time MR temperature mapping in the brain: A comparison of fast sequences. Physica Medica. 2010.
63. Gardener AG, Francis ST. Multislice perfusion of the kidneys using parallel imaging: Image acquisition and analysis strategies. Magnetic Resonance in Medicine. 2010;63(6):1627-36.
64. Goerke U, Ugurbil K. Robust detection of functional activation in the superior colliculus without ECG-triggering. Proceedings of the international society of magnetic resonance in medicine. 2009;17:19.

65. Hofstetter L, Yeo D, Dixon W, Davis C, Foo T, editors. Fat-Referenced MR Themometry Using 3-Echo Phase-based Fat water separation Method. ISMRM Annual Meeting; 2011; Montreal, Canada.

66. Cannon B, Nedergaard J. Brown adipose tissue: function and physiological significance. Physiol Rev. 2004;84(1):277-359.

67. Bousquet JC, Saini S, Stark DD, Hahn PF, Nigam M, Wittenberg J, et al. Gd-DOTA: characterization of a new paramagnetic complex. Radiology. 1988;166(3):693-8.

68. Shrivastava D, Hanson T, Kulesa J, DelaBarre L, Iaizzo P, Vaughan JT. Radio frequency heating at 9.4T (400.2 MHz): in vivo thermoregulatory temperature response in swine. Magn Reson Med. 2009;62(4):888-95.

69. Shrivastava D, Schlentz R, Kulesa J, DelaBarre L, Snyder C, Hanson T, et al., editors. Identification of Possibly Unsafe RF Exposure Thresholds for Humans using Porcine Models. ASME-SBC; 2008; ASME - Summer Bioengineering Conference, Marco Island, USA, 2008.

70. Vaughan T, DelaBarre L, Snyder C, Tian J, Akgun C, Shrivastava D, et al. 9.4T human MRI: preliminary results. Magn Reson Med. 2006;56(6):1274-82.

71. Shrivastava D, DelaBarre L, Michaeli S, Snyder C, Hanson T, Vaughan JT, editors. Proton Resonance Frequency Shift Based NMR Thermometry for Ultra-High Field RF Safety Applications.2008; Proceedings of the International Society of Magnetic Resonance in Medicine, Toronto, Canada.

72. Shrivastava D, DelaBarre L, Hanson T, Vaughan JT, editors. Improved MR Thermometry to Measure Brain Temperatures2008; ASME - Summer Bioengineering Conference, Marco Island, USA.